

Scaling of the $\gamma p \rightarrow \pi^0 p$ process from the Regge pole exchange with nucleon resonances

Kook-Jin Kong*

Research Institute of Basic Sciences, Korea Aerospace University, Goyang, 10540, Korea

Tae Keun Choi†

Department of Physics, Yonsei University, Wonju, 26493, Korea

Byung-Geel Yu‡

Research Institute of Basic Sciences, Korea Aerospace University, Goyang, 10540, Korea

We have investigated photoproduction of neutral pion $\gamma p \rightarrow \pi^0 p$ process with N^* and Δ resonances included in the Regge theory up to photon energy $E_\gamma = 3$ GeV. Given the Regge pole exchanges $\rho(770) + \omega(780) + b_1(1235) + h_1(1170)$ for the background contribution which agrees with high energy data in the Regge realm, the resonances of the Breit-Wigner form as the four-star rank are introduced to estimate total and differential cross sections together with beam asymmetry Σ . The differential cross section $s^7 d\sigma/dt$ scaled by energy are reproduced to agree with the recent Jefferson Lab data, revealing the production mechanism of the big bump structure around $W \approx 2.2$ GeV by the diffractive pattern of the ω exchange that originates from the zeros of the trajectory $\alpha_\omega(t) = 0$ in the canonical phase, $\frac{1}{2}(-1 + e^{-i\pi\alpha_\omega(t)})$.

PACS numbers: 12.38.Lg, 11.55.Jy, 13.75.Gx, 13.60.Le

Keywords: scaling, scaled cross section, π^0 photoproduction, ω -meson, Regge model, Breit-Wigner resonance

It is believed that hadrons consist of quarks and gluon and their interactions are governed by quantum chromodynamics (QCD). Due to the quark confinement, however, hadronic processes are usually described by meson and nucleon degrees of freedom. In this respect, it would be of interest to observe the evidence for the quark and gluon degrees of freedom through exclusive hadronic processes.

Recent experiments on pion photoproduction at the Jefferson Lab [1–3] have opened such a possibility by measuring the differential cross section at high energy and large momentum transfer which is predicted to obey the scaling, i.e.,

$$\frac{d\sigma}{dt} \sim F(t/s) s^{2-n}, \quad (1)$$

by the quark-counting rule [4, 5]. Here n is the number of constituents (gauge boson plus the quarks) participating in the process at the fixed angle in the c.m. frame. For the pion photoproduction, $n = 9$, and, therefore, the measured cross sections from the CLAS glc collaboration are expected to show such a scaling behavior $s^7 d\sigma/dt \sim F(t_0/s) \sim \text{constant}$ at the fixed angle $\theta = 90^\circ$ (or fixed t_0) as energy increases.

In this letter we investigate the process $\gamma p \rightarrow \pi^0 p$ with a focus on understanding the origin of the scaling at the level of hadronic degrees of freedom. As the issue requires a model capable of describing the process at high energy we shall work with the t -channel Regge pole exchanges. Moreover since the scaled cross section in the

low energy region shows an oscillatory behavior which may be due to the resonance peaks we consider an incorporation of the N^* and Δ resonances with the Regge theory. We recall that the Regge pole is a partial wave amplitude analytically continued in the angular momentum space, it is good to start from the resonance of the Breit-Wigner (BW) form for the partial wave of a specific angular momentum and parity eigenstate in the production amplitude.

In the neutral process where π^0 exchange is forbidden by charge-conjugation, $\omega(780)$, $\rho(770)$, $h_1(1170)$, and $b_1(1235)$ Regge poles are considered in the t -channel exchange to serve as a background contribution. Then, the whole amplitude will be composed of the t -channel Regge poles and the nucleon resonance R of spin- J possible to the process, i.e.,

$$\mathcal{M} = -\mathcal{M}_{\text{Regge}} - \sum_{R=\Delta} \mathcal{M}_R^J - \sum_{R=N^*} \mathcal{M}_R^J. \quad (2)$$

In table I the coupling constants and the Regge trajectories are summarized with the detailed expression for the $\mathcal{M}_{\text{Regge}}$ given in Ref. [6]. Here, we consider the resonances that are ranked as the four-star in Particle Data Group (PDG) for definiteness sake. For each resonance the partial amplitude is described by the helicity ampli-

TABLE I. Coupling constants and trajectories for Regge poles. $g_{\gamma\pi V}$ is given in unit of GeV^{-1} .

meson	trajectory	phase	$g_{\gamma\pi V}$	g_{VNN}^v	g_{VNN}^t
ρ	$0.8t + 0.55$	$e^{-i\pi\alpha_\rho}$	0.255	2.6	16.12
ω	$0.9t + 0.44$	$\frac{-1+e^{-i\pi\alpha_\omega}}{2}$	0.723	15.6	0
b_1	$0.7(t - m_{b_1}^2) + 1$	1	0.189	0	-14
h_1	$0.7(t - m_{h_1}^2) + 1$	1	0.405	0	-14

* kong@kau.ac.kr

† tkchoi@yonsei.ac.kr

‡ bgyu@kau.ac.kr

tude of Ref. [7] with the definition and the sign convention of the electric and magnetic multipoles further from Ref. [8, 9] in relation with the CGLN amplitude. Then, the resonance R of spin- J is written as

$$\mathcal{M}_R^J = \sum_{i=1}^4 H_i^J(W, \theta), \quad (3)$$

where the angular dependence of the amplitude H_i^J is expressed in the helicity formulation as in Ref. [7] with its energy-dependence given by the electric and magnetic multipoles [10],

$$E_{l\pm} = \frac{\beta_E}{\sqrt{q_R k_R j_\gamma(j_\gamma + 1)}} \frac{M_R \sqrt{\Gamma_{R\gamma N} \Gamma_{R\pi N}}}{M_R^2 - s - iM_R \Gamma} e^{-d\epsilon_R^2}, \quad (4)$$

$$M_{l\pm} = \frac{\beta_M}{\sqrt{q_R k_R j_\gamma(j_\gamma + 1)}} \frac{M_R \sqrt{\Gamma_{R\gamma N} \Gamma_{R\pi N}}}{M_R^2 - s - iM_R \Gamma} e^{-d\epsilon_R^2}, \quad (5)$$

respectively. Note that the electromagnetic (EM) multipoles in Eqs. (4) and (5) are different from those of Ref. [10] in that the decay widths of resonance $R \rightarrow \gamma N$ and $R \rightarrow \pi N$ reported in the PDG are employed instead of Γ_E , Γ_M and $\Gamma_{l\pm}$ in Ref. [10], because it is convenient to utilize the decay widths known for $R \rightarrow \gamma N$ and $R \rightarrow \pi N$ for use.

In the application we use the β_E and β_M which are determined at the resonance position $W = M_R$ by using Eqs. (4) and (5), in which case the EM multipoles $E_{l\pm}(M_{l\pm})$ and $\Gamma_{R\gamma N}$ are estimated at $W = M_R$ as follows [8]; Given the values of the helicity amplitudes $A_{1/2}$ and $A_{3/2}$ known for $l+$ multipole amplitudes,

$$A_{1/2} = -\frac{1}{2} [(l+2)\mathcal{E}_{l+} + l\mathcal{M}_{l+}], \quad (6)$$

$$A_{3/2} = \frac{\sqrt{l(l+2)}}{2} [\mathcal{E}_{l+} - \mathcal{M}_{l+}], \quad (7)$$

and for $(l+1)-$ multipole amplitudes,

$$A_{1/2} = \frac{1}{2} [(l+2)\mathcal{M}_{(l+1)-} - l\mathcal{E}_{(l+1)-}], \quad (8)$$

$$A_{3/2} = -\frac{\sqrt{l(l+2)}}{2} [\mathcal{E}_{(l+1)-} + \mathcal{M}_{(l+1)-}], \quad (9)$$

the multipoles $\mathcal{E}_{l\pm}(M_{l\pm})$, and $E_{l\pm}(M_{l\pm})$ can be determined at $W = M_R$, which are related by

$$\text{Im} E_{l\pm}(M_{l\pm}) = a \mathcal{E}_{l\pm}(\mathcal{M}_{l\pm}), \quad (10)$$

with

$$a = C_I \left[\frac{1}{(2J+1)\pi} \frac{k_R}{q_R} \frac{M_N}{M_R} \frac{\beta_{\pi N}}{\Gamma} \right]^{1/2}, \quad (11)$$

$$C_{1/2} = -\sqrt{\frac{1}{3}}, \quad C_{3/2} = \sqrt{\frac{2}{3}}. \quad (12)$$

Here $\beta_{\pi N}$ is the branching ratio of the resonance to the πN channel, Γ , M_R , J and I are the total width, mass, spin, isospin of the resonance R , k_R and q_R are momenta of photon and pion at the resonance position in the c.m.

system. C_I is the Clebsch-Gordan coefficient and M_N is the nucleon mass. With the known values for $A_{1/2}$ and $A_{3/2}$ the partial width $R \rightarrow \gamma N$ in Eqs. (4) and (5) is obtained as well from the equation,

$$\Gamma_{R\gamma N} = \frac{k_R^2}{\pi} \frac{2M_N}{(2J+1)M_R} [|A_{1/2}|^2 + |A_{3/2}|^2]. \quad (13)$$

In relation with Ref. [10], we write

$$\Gamma_{E(M)} \Gamma_{l\pm} = \beta_{E(M)}^2 \Gamma_{R\gamma N} \Gamma_{R\pi N}. \quad (14)$$

From Eq. (14) the $\beta_E(\beta_M)$ estimated as discussed above, thus, provides the information about the case of coupling of the electric (magnetic) photon in the model of Ref. [10]. For a better description of the resonance we now introduce the cutoff factor $e^{-d\epsilon_R^2}$ to adjust the range of the resonance by a dimensionless parameter d together with $\epsilon_R = \frac{M_R^2 - s}{M_R \Gamma}$ [11]. Therefore, we have no parameters except for the d within the present framework where M_R , Γ , $\beta_{\pi N}$, and $A_{1/2}$ and $A_{3/2}$ are to be taken from PDG.

Before proceeding we wish to give a comment on the possibility of double-counting by the duality of the t -channel Regge poles to the s -channel resonances which is expressed as the finite energy sum rule [12]. From the superconvergence of the amplitude [13] we briefly assume in Eq. (2), the sum rule reads

$$\frac{1}{s} \int^s ds' \text{Im} \sum_R \mathcal{M}_R^J = \sum_{i=\rho, \omega} \frac{\gamma_i(t)}{\Gamma(\alpha_i(t)) \alpha_i(t)} s^{\alpha_i(t)-1} \quad (15)$$

for ρ and ω of only the complex phase in table I chosen for the present process. The $\gamma_i(t)$ stands for the residue of the vector meson exchange in the $\mathcal{M}_{\text{Regge}}$ including the product of the couplings $\gamma\pi V$ and VNN . Thus, the double-counting by the t -channel comes from the $\rho + \omega$ Regge pole which, however, amounts to several percent

TABLE II. Physical constants for Δ and N^* resonances. Widths and masses are given in units of MeV, $A_{1/2}$, $A_{3/2}$ are given in unit of $\text{GeV}^{-1/2}$.

Resonance	J^P	M_R	Γ	$A_{1/2}$	$A_{3/2}$	$\beta_{\pi N}$	d
$\Delta(1232)$	$(3/2)^+$	1220	130	-0.13	-0.26	1.0	0.05
$N(1440)$	$(1/2)^+$	1400	190	-0.08	0.0	0.75	0.25
$N(1520)$	$(3/2)^-$	1505	120	-0.007	0.168	0.65	0.1
$N(1535)$	$(1/2)^-$	1515	150	0.13	0.0	0.55	0.25
$\Delta(1620)$	$(1/2)^-$	1590	120	0.055	0.0	0.3	0.25
$N(1650)$	$(1/2)^-$	1670	120	0.065	0.0	0.7	0.1
$N(1675)$	$(5/2)^-$	1660	135	0.01	0.015	0.35	0.2
$N(1680)$	$(5/2)^+$	1675	110	-0.01	0.10	0.675	0.1
$\Delta(1700)$	$(3/2)^-$	1675	250	0.12	0.12	0.15	0.25
$N(1720)$	$(3/2)^+$	1680	250	0.07	0.15	0.1	0.1
$\Delta(1905)$	$(5/2)^+$	1900	280	0.025	-0.04	0.1	0.2
$\Delta(1910)$	$(1/2)^+$	1885	220	0.06	0.0	0.3	0.25
$\Delta(1950)$	$(7/2)^+$	1890	240	-0.02	-0.10	0.35	0.1
$N(2190)$	$(7/2)^-$	2150	450	-0.065	0.035	0.1	0.2
$N(2220)$	$(9/2)^+$	2250	400	0.01	0.01	0.2	0.2
$N(2250)$	$(9/2)^-$	2275	500	0.01	0.01	0.1	0.2

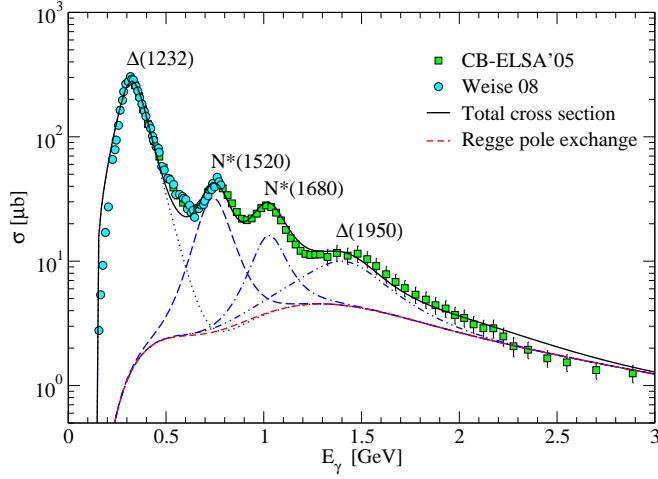


FIG. 1. (Color online) Total cross section for $\gamma p \rightarrow \pi^0 p$ from threshold to $E_\gamma = 3$ GeV. Red dashed line is the background from $\rho + \omega + b_1 + h_1$ Regge pole exchanges. Black solid line results from the background plus the resonances. Four non-solid lines corresponding to the respective contributions of $\Delta(1232)$, $N(1520)$, $N(1680)$, and $\Delta(1950)$ are illustrated to represent the sequential peaks. Data are taken from Refs. [3, 14].

of the cross section at most, as can be seen in Fig. 1. Hence, we here neglect the double-counting due to the t -channel Regge poles.

With the physical constants listed in table II which are within the range of PDG values, we present the total cross section in Fig. 1 up to $E_\gamma = 3$ GeV where the contributions of the resonances, $\Delta(1232)$, $N(1520)$, $N(1680)$, and $\Delta(1950)$ are shown to represent the four prominent peaks, respectively. In the Regge realm beyond $E_\gamma = 3$ GeV, of course, the cross section coincides with that from the pure Regge pole exchanges as described in Ref. [6].

Figures 2 and 3 show the differential cross sections and the beam asymmetries reproduced at four energy bins each of which corresponds to the region around $\Delta(1232)$, $N(1520)$, $N(1680)$, and $\Delta(1950)$, respectively. The results are obtained through an optimal compromise between cross sections for total, differential, and beam asymmetry to agree with experimental data. Near the first resonance peak $W \approx 1232$ MeV, it is enough to consider $\Delta(1232)$ to describe the differential cross section and beam asymmetry. In the second resonance region mainly due to $N(1520)$, the resonances $N(1440)$ and $N(1535)$ are added to agree with the beam asymmetry Σ . To reproduce the differential cross section at the third peak due to $N(1680)$, the resonance $\Delta(1700)$ together with $N(1650)$ play the role to fit to Σ . Around the fourth peak, apart from $\Delta(1950)$ which is most representative one to cover this region, $\Delta(1910)$ is considered to give a contribution to Σ .

Let us now discuss the feature of the differential cross section scaled by s^7 within the present framework which

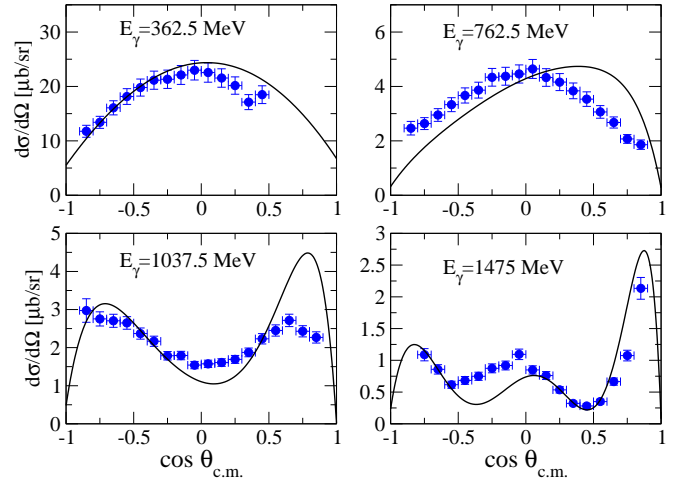


FIG. 2. (Color online) Differential cross sections for $\gamma p \rightarrow \pi^0 p$ in four energy bins $E_\gamma = 362.5$ ($W = 1249.2$), 762.5 (1520.3), 1037.5 (1681.5) and 1475 (1910) MeV. Data are taken from Refs. [15, 16].

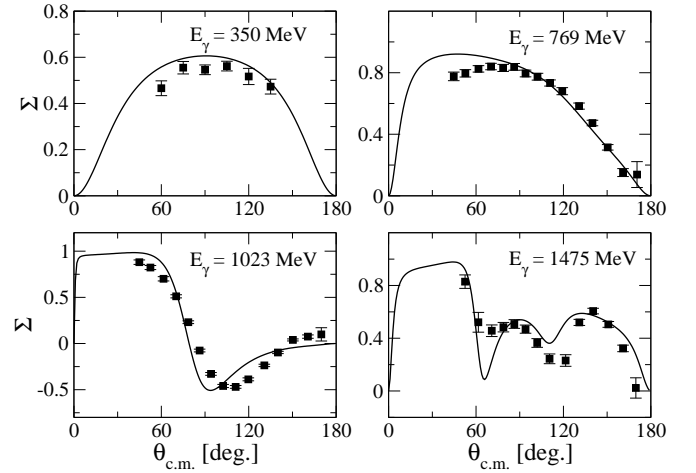


FIG. 3. Angular distribution of the beam asymmetry Σ for $\gamma p \rightarrow \pi^0 p$ in four energy bins $E_\gamma = 350$ ($W = 1240$), 769 (1524), 1023 (1673) and 1475 (1910) MeV. Data are taken from Refs. [15, 16].

has been validated as discussed above. Figure 4 shows three scaled cross sections the first of which reproduces existing data at the angle $\theta = 90^\circ$, while the other two are predicted at $\theta = 70^\circ$ and 50° , respectively. It is certain that the oscillatory behavior below $W \approx 2$ GeV is due to the resonances $\Delta(1232)$, $N(1520)$, and $N(1680)$ in order. Within the Regge framework where the production mechanism of the π^0 process is dominated by the ω exchange [6, 17], the bump structure around $W \approx 2.2$ GeV, in essence, results from the diffractive pattern arising from the nonsense wrong signature zero (NWSZ) of the ω trajectory $\alpha_\omega(t) = 0$. This in fact leads to the vanishing of the amplitude at $W \approx 1.58$ GeV at the angle $\theta = 90^\circ$, as shown in Fig. 5. While the cross section is suppressed in the low energy but amplified at high energy

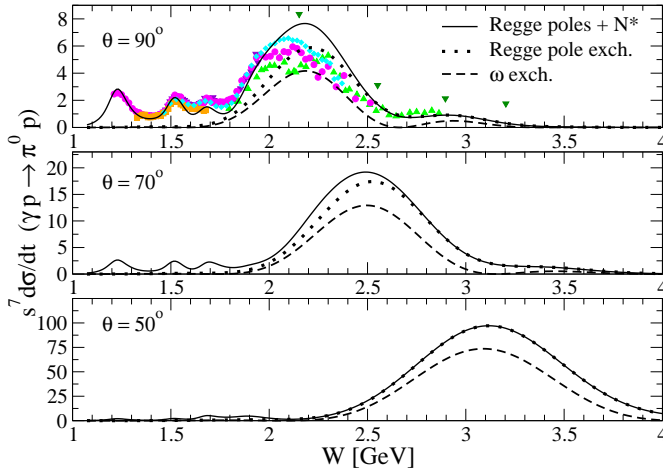


FIG. 4. (Color online) Scaled cross section $s^7 \frac{d\sigma}{dt}$ ($10^7 \text{ GeV}^{14} \text{ nb/GeV}^2$) for $\gamma p \rightarrow \pi^0 p$ at $\theta = 90^\circ$, $\theta = 70^\circ$, and $\theta = 50^\circ$ as a function of total energy W . N^* contributions vanish at $\theta = 50^\circ$. Data are taken from Refs. [2, 3, 18–21].

by the s^7 -scale, the shift of the bump to the position $W \approx 2.5$ GeV at $\theta = 70^\circ$, and to 3.1 GeV at $\theta = 50^\circ$ in Fig. 4 can, thus, be understood as the result of a sequential shift of the NWSZ to $W \approx 1.75$ GeV, and to 2.11 GeV accompanying with the diffractive pattern according to the change of the angle. The resonances $N(2190)$, $N(2220)$, and $N(2250)$ are shown in Fig. 4 to contribute to the bump structure in the scaled cross section at $\theta = 90^\circ$, which, nevertheless, vanish by degrees without affecting the structure of the bump as the angle becomes forward directional. This confirms what we have analyzed for the production mechanism of the bump structure.

In summary, we have investigated the $\gamma p \rightarrow \pi^0 p$ process with a view to understanding the bump structure not expected from nucleon resonances but observed in the scaled cross section $s^7 d\sigma/dt$. For a reliable discussion

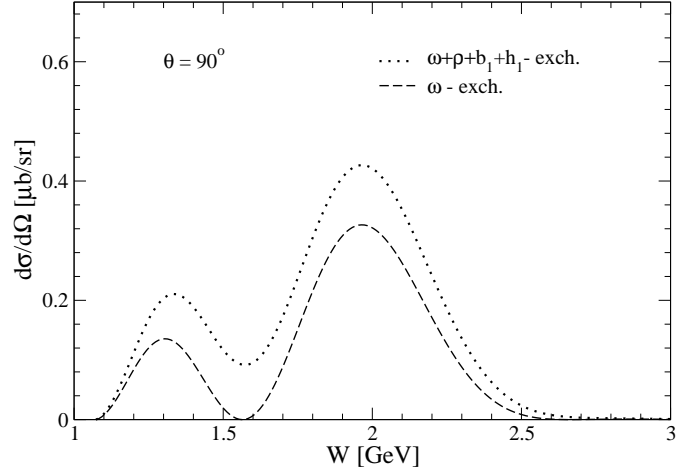


FIG. 5. Diffractive pattern of the differential cross section $\frac{d\sigma}{d\Omega}$ at $\theta = 90^\circ$ for $\gamma p \rightarrow \pi^0 p$ with a dip at $W = 1.58$ GeV by NWSZ of the ω -trajectory (dashed line).

on this issue we have constructed a model which incorporates the nucleon resonances with the t -channel Regge pole exchange based on the helicity amplitude. With the parameter d only varied to adjust the range of a resonance total and differential cross sections as well as the beam asymmetry are shown to agree at the optimal compromise with the three sets of experimental data. It is pointed out that the big bump structure originates substantially from the diffractive pattern by the NWSZ of the ω -meson exchange in the scaled differential cross section.

ACKNOWLEDGMENT

This work was supported by the grant NRF-2013R1A1A2010504 from National Research Foundation (NRF) of Korea.

-
- [1] L. Y. Zhu *et al.*, Phys. Rev. Lett. **91**, 022003 (2003); Phys. Rev. C **71**, 044603 (2005).
 - [2] M. Dugger, *et al.*, Phys. Rev. C **76**, 025211 (2007).
 - [3] O. Bartholomy, *et al.*, Phys. Rev. Lett. **94**, 012003 (2005).
 - [4] S. J. Brodsky and G. R. Farrar, Phys. Rev. Lett. **31**, 1153 (1973).
 - [5] G. P. Lepage, and S. J. Brodsky, Phys. Rev. D **22**, 2157 (1980).
 - [6] B. G. Yu, T. K. Choi, and W. Kim, Phys. Rev. C **83**, 025208 (2011).
 - [7] R. L. Walker, Phys. Rev. **182**, 1729 (1969).
 - [8] I. G. Aznauryan, V. D. Burkert, and T.-S. H. Lee, arXiv:0810.0997.
 - [9] D. Drechsel, L. Tiator, J. Phys. G **18**, 449 (1992).
 - [10] H. Thom, Phys. Rev. **151**, 1322 (1966).
 - [11] A. J. Lennox *et al.*, Phys. Rev. D **11**, 1777 (1975).
 - [12] H. Harari, Phys. Rev. Lett. **20**, 1395 (1968).
 - [13] K. Igi and S. Matsuda, Phys. Rev. **163**, 1622 (1967).
 - [14] M. Weis *et al.*, Eur. Phys. J. A **38**, 27 (2008).
 - [15] O. Bartalini, *et al.*, Eur. Phys. J. A **26**, 399 (2005).
 - [16] A. A. Belyaev, *et al.*, Nucl. Phys. B **213**, 201 (1983).
 - [17] M. Guidal, J.-M. Laget, and M. Vanderhaeghen, Nucl. Phys. A **627**, 645 (1997).
 - [18] O. Bartalini, *et al.*, Eur. Phys. J. A **26**, 399 (2005).
 - [19] A. Imanishi, *et al.*, Phys. Rev. Lett. **54**, 2497 (1985).
 - [20] M. A. Shupe, *et al.*, Phys. Rev. D **19**, 1921 (1979).
 - [21] R. Alvarez, *et al.*, Phys. Rev. Lett. **12**, 707 (1964).